4

All-Poly-Crystalline Ceramics Nd:YAG/Cr^{4+}:YAG Monolithic Micro-Lasers with Multiple-Beam Output

Nicolaie Pavel[1,2], Masaki Tsunekane[1] and Takunori Taira[1]
[1]*Institute for Molecular Science (IMS), Laser Research Center, 38 Nishigonaka, Myodaiji, Okazaki*
[2]*National Institute for Laser, Plasma and Radiation Physics, Solid-State Quantum Electronics Lab., Bucharest*
[1]*Japan*
[2]*Romania*

1. Introduction

Laser-induced ignition of air-fuel mixtures in internal combustion engines is a subject that has been investigated extensively during last years. In the beginning, experiments were performed with sized and robust, commercial available lasers that delivered pulses with energy in the range of tens to a few hundreds of mJ and several ns pulse duration (Ma et al., 1998; Phuoc & White, 1999; Weinrotter et al. 2005a; Weinrotter at al. 2005b). These investigations revealed that laser-induced ignition offers significant advantages over a conventional spark-ignition system, such as higher probability to ignite leaner mixtures, reduction of erosion effects, increase of engine efficiency, or shorter combustion time. Thus, developing of an engine ignited by laser could address, even partially, the increase concern of humanity for protecting global environment and preserving fossil resources.
Subsequent research (Kofler et al., 2007) concluded that a suitable laser configuration for engine ignition is a Nd:YAG laser, passively Q-switched by Cr^{4+}:YAG saturable absorber (SA). Q-switched laser pulses with energy up to 6 mJ and 1.5-ns duration were obtained from an end-pumped, 210-mm long Nd:YAG-Cr^{4+}:YAG laser. Furthermore, side-pumping technique was employed to realize a Nd:YAG laser passively Q-switched by Cr^{4+}:YAG SA with 25 mJ energy per pulse and pulse duration around 3 ns (Kroupa et al. 2009); the laser resonator was around 170 mm. However, the length of these lasers make difficult to accomplish compactness of an electrical spark plug used in the automotive industry.
In recent works our group has realized Nd:YAG-Cr^{4+}:YAG micro-lasers and demonstrated laser ignition of an automobile engine with improved performances in comparison with ignition induced by a conventional spark plug (Tsunekane at al. 2008; Tsunekane et al. 2010). The strategy was to shorten the pulse duration by decreasing the resonator length, and to maximize the laser pulse energy by optimizing the pump conditions, the Nd:YAG doping level and length, as well as Cr^{4+}:YAG initial transmission (T_0) and the output mirror transmission (T) (Sakai et al., 2008). A passively Q-switched Nd:YAG-Cr^{4+}:YAG micro-laser with 2.7-mJ energy per pulse and 600-ps pulse duration was realized. This laser, which

included optics for pumping, an 11-mm long resonator, as well as optics that collimated and focused the beam to dimension required for fuel ignition, was assembled in a device that matched the dimensions of an electrical spark plug (Tsunekane at al., 2010).
Various papers have also reported that multi-point ignition increases significantly the combustion pressure and shortens the combustion time compared to single-point ignition (Weinrotter et al., 2005a; Phuoc, 2000; Morsy et al., 2001). The experiments employed combustion chambers in which two laser beams were inserted through different windows, and thus distance between the ignition points was adjusted easily. However, the use of a single laser beam that was focused in three points with a diffractive lens failed to demonstrate improved combustion (Weinrotter et al., 2005a), opposite to the two-point ignition experiments. The result was attributed to the short distance between the ignition points. Therefore, study of the influence of multi-point ignition on the performances of a real car engine would require realization of passively Q-switched Nd:YAG/Cr^{4+}:YAG lasers with multiple-beam output and with size close to that of an electrical spark plug.
In this work we report passively Q-switched Nd:YAG/Cr^{4+}:YAG micro-lasers with multiple (two and three)-beam output, each beam inducing air-breakdown in points at adjustable distance. Opposite to the previous realized lasers that used discrete Nd:YAG and Cr^{4+}:YAG single-crystals components (Koefler et al., 2007; Kroupa et al., 2009; Tsunekane et al., 2008; Tsunekane at al., 2010; Sakai et al., 2008), these lasers consist of composite, all-ceramics Nd:YAG/Cr^{4+}:YAG monolithic media that were pumped by similar, independent lines.
This work is organized as follows. Section 2 presents a continuous-wave (cw) pumped Nd:YAG laser passively Q-switched by Cr^{4+}:YAG SA with emission at 1.06 μm. Although the laser pulse energy (E_p) was low, of 270 μJ at the repetition rate of ~9 KHz, and the pulse peak power was of only 16 kW, this device was the first passively Q-switched laser realized in our laboratory. Furthermore, it was used to demonstrate the first passively Q-switched Nd:YAG-Cr^{4+}YAG laser with generation into green visible spectrum at 532 nm by intracavity frequency doubling with LiB_3O_5 (LBO) nonlinear crystal. In these experiments, both active Nd:YAG gain medium and Cr^{4+}:YAG SA were of single-crystal nature. Section 3 is dedicated to repetitively-pumped, passively Q-switched Nd:YAG-Cr^{4+}:YAG lasers with high pulse energy and few-MW level peak power. Results obtained with single-crystals, Nd:YAG and Cr^{4+}:YAG discrete elements are given in Section 3.1. A detailed investigation of laser emission obtained with ceramics Nd:YAG and Cr^{4+}:YAG was performed (Section 3.2): This was a step toward establishing ceramics materials as solution for a microchip laser used in laser ignition of an engine. Lastly, composite, all-ceramics Nd:YAG/Cr^{4+}:YAG monolithic laser with two- and three-beam output were realized. Various characteristics of these devices are given and discussed in Section 3.3. The paper conclusions are presented in Section 4. The lasers described in this work will enable studies on the performances of internal combustion engines with multi-point ignition.

2. Infrared at 1.06 μm and green at 532 nm passively Q-switched Nd:YAG lasers

Passive Q-switching technique is attractive particularly for scientific, medical, or industrial applications that do not require temporal accuracy better than microseconds range. This method yields lower output compared to electro-optic or acousto-optic Q-switched lasers, but has the advantages of a simple design, with good efficiency, reliability and compactness. The first cw, diode end-pumped Nd:YAG laser passively Q-switched by Cr^{4+}:YAG SA

crystal delivered pulses with 11-μJ energy and 337-ps duration, at 6-kHz repetition rate (Zayhowsky and Dill III, 1994). The laser included a composite structure that was made of a thin piece of Nd^{3+}:YAG single-crystal gain medium bonded to a short Cr^{4+}:YAG SA single crystal. Later, laser pulses with increased energy of 100 μJ and duration of 36 ns at 15-kHz repetition rate were obtained from a passively Q-switched Nd:YAG-Cr^{4+}:YAG laser, with medium average output power (Agnesi et al., 1997). Furthermore, laser pulses with high energy E_p= 3.4 mJ, but long duration of 99 ns, were achieved by employing side-pumping geometry of a Nd:YAG-Cr^{4+}:YAG laser (Song et al., 2000).
A sketch of the cw-pumped Nd:YAG-Cr^{4+}:YAG laser developed in our laboratory is shown in Fig. 1 (Pavel et al., 2001a). The gain medium was a composite Nd:YAG rod that was fabricated by diffusion bonding of a Nd:YAG single crystal (thickness of 5.0 mm, 1.1-at.% Nd doping) to an undoped, 1.0-mm thick YAG. The concept of combining doped and undoped components was used, in the beginning, to modify the configuration of the thermal field induced by pumping in solid-state laser rods, and successfully employed to improve the output performances of Nd:YAG (Hanson, 1995), Nd:YVO_4 (Tsunekane et al., 1997), or Yb:YAG (Bibeau et al., 1998) lasers. This method has also found applications in the passive Q-switching technique. Thus, microchip structures that consisted of undoped YAG caps, Nd:YAG and Cr^{4+}:YAG SA bonded together to form a monolithic resonator were demonstrated to produce linearly polarized, single-longitudinal mode output pulses in quasi-cw or pulsed pumping regimes (Zayhowski et al., 2000; Aniolek et al., 2000).

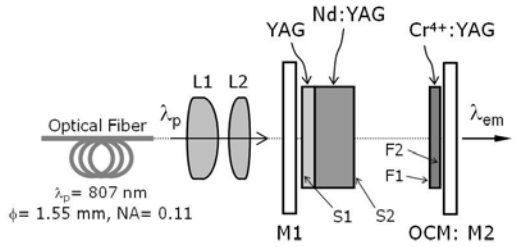

Fig. 1. A passively Q-switched Nd:YAG-Cr^{4+}:YAG laser, pumped by cw diode laser is shown. Composite YAG/Nd:YAG was used for thermal management. The gain Nd:YAG medium as well as Cr^{4+}:YAG SA were single crystals, discrete elements.

A fiber-bundled diode (OPC-B030-mmm-FC, OptoPower Co.; 1.55-mm diameter, 0.11 NA) was used for the pump at 807 nm (λ_p). The YAG/Nd:YAG surfaces (S1 and S2) were antireflection (AR) coated at both the laser wavelength of 1.064 μm (λ_{em}) and λ_p. A plane-plane resonator with the pump-mirror M1 coated for high reflectivity (HR) at λ_{em} and high transmission (HT) at λ_p, and that was placed very close to Nd:YAG, was used. A collimating lens (L1) and a focusing lens (L2) were used to image the fiber bundle end into Nd:YAG, to a diameter of 800 μm. The focusing point was 2.0 mm below surface S1 of Nd:YAG. Cr^{4+}:YAG SA (CASIX Inc., China) with initial transmission T_0 of 0.89, 0.85, and 0.80 and AR coated at λ_{em} on both surfaces (F1 and F2) were used for Q-switching. Each Cr^{4+}:YAG SA crystal was placed close to the out-coupling mirror (OCM) M2.
Figure 2 presents characteristics of Q-switched laser emission obtained from a 40-mm long resonator and an OCM with T= 0.10. A maximum average power of 3.8 W resulted for the Cr^{4+}:YAG with T_0= 0.89 (Fig. 2a) with a beam factor M^2 of 1.4. The laser ran at a frequency as

high as 24.8 kHz. The pulse energy and the pulse duration (t_p, FWHM definition) were E_p= 152 μJ and t_p= 25.4 ns (Fig. 2b), respectively; the pulse peak power was ~6.0 kW. When a SA with a lower transmission T_0 was used, pulses with higher peak power were generated with a reduced average output power. For a Cr^{4+}:YAG SA with T_0= 0.85, pulses with t_p= 18.0 ns at a repetition rate of 16.1 kHz resulted for the maximum absorbed power of 21.0 W. Energy E_p and pulse peak power was 213 μJ and 11.8 kW, respectively. For a Cr^{4+}:YAG with T_0= 0.80 an average power of 2.6 W at the absorbed pump power of 18.6 W resulted. The laser ran at 9.1 kHz repetition rate with pulses of E_p= 272 μJ energy and 16.2 kW peak power.

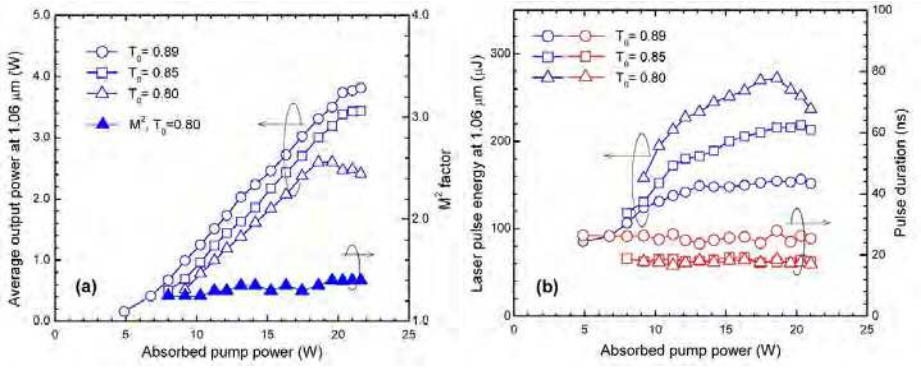

Fig. 2. Cw pumped, passively Q-switched Nd:YAG-Cr^{4+}:YAG laser: (a) Average output power and the laser-beam M^2 factor; (b) Laser pulse energy and laser pulse duration.

The Q-switched laser performances were evaluated with a rate equation model (Pavel et al., 2001a; Degnan, 1995; Zhang et al., 1997). The laser pulse energy is given by general relation:

$$E_p = \frac{h\nu \cdot A_g}{2\gamma_g \sigma_g} \cdot \ln R \cdot \ln\left(\frac{n_{gf}}{n_{gi}}\right) \tag{1}$$

where hν is the photon energy at 1.06 μm, σ_g represents Nd:YAG stimulated emission, γ_g is the inversion reduction factor, A_g is the effective area of the laser beam in Nd:YAG, and the OCM reflectivity is R= (1-T). The initial population inversion density, n_{gi} is:

$$n_{gi} = \frac{-\ln R + L - \ln T_0^2}{2\sigma_g \ell_g} \tag{2}$$

where L represents the resonator round-trip residual loss and ℓ_g is the Nd:YAG length. The final population inversion density, n_{gf} and n_{gi} are related by equation:

$$\left(1 - \frac{n_{gf}}{n_{gi}}\right) + \left[1 + \frac{(1-\delta)\cdot \ln T_0^2}{(-\ln R + L - \ln T_0^2)}\right] \cdot \ln\left(\frac{n_{gf}}{n_{gi}}\right) + \frac{1}{\alpha} \cdot \frac{(1-\delta)\cdot \ln T_0^2}{(-\ln R + L - \ln T_0^2)} \cdot \left[1 - \left(\frac{n_{gf}}{n_{gi}}\right)^{\alpha}\right] = 0 \tag{3}$$

$\delta = \sigma_{ESA}/\sigma_{SA}$, with σ_{SA} and σ_{ESA} the absorption cross section and exited-state absorption cross section of Cr^{4+}:YAG, respectively. Parameter α is $\alpha = (\gamma_{SA}\sigma_{SA})/(\gamma_g\sigma_g)\times(A_g/A_{SA})$; γ_{SA} is the inversion reduction factor for Cr^{4+}:YAG and A_{SA} is the laser beam effective area in Cr^{4+}:YAG.

Figure 3 compares experimental (symbols) and calculated (continuous lines) pulse energy for two pump rates. In simulation, spectroscopic parameters of Nd:YAG and Cr^{4+}:YAG were $\sigma_g = 2.3\times10^{-19}$ cm^2 , $\sigma_{SA} = 4.3\times10^{-18}$ cm^2, and $\sigma_{ESA} = 8.2\times10^{-19}$ cm^2 (Shimony, et al., 1995). The laser beam sizes in the gain crystal and in Cr^{4+}:YAG were evaluated by the PARAXIA software package (Sciopt Enterprises, San Jose, California), in which the active medium was described as a thin lens. For the absorbed power of 9.2 W (near to the threshold) the calculated active element focal length was 33.8 cm and the ratio A_g/A_{SA} amounted to 1.1, while for the absorbed pump power of 17.5 W (close to the maximum pump power) the focal length decreases to 13.2 cm and A_g/A_{SA} was 1.3. Good agreement between the experimental results and the calculated values was obtained.

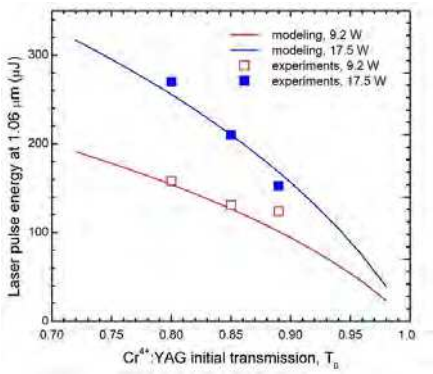

Fig. 3. Laser pulse energy versus transmission T_0 of Cr^{4+}:YAG. Symbols are experimental data (open and filled signs for absorbed pump power of 9.2 W and 17.5 W, respectively), whereas lines represent modeling.

In order to realize a passively Q-switched Nd:YAG-Cr^{4+}:YAG laser with generation into green visible spectrum at 532 nm ($\lambda_{2\omega}$), the set-up of Fig. 1 was modified such to include a nonlinear crystal. We used a V-type resonator, as shown in Fig. 4 (Pavel et al., 2001b). The YAG/Nd:YAG crystal, the Cr^{4+}:YAG SA and a glass plate (BP) positioned at Brewster angle for polarization were placed in the resonator arm (of 80-mm length) made between mirrors M1 and M2. The nonlinear crystal was a 10-mm long LBO (type I, $\theta = 90^0$, $\phi = 11.4^0$; operation at 25^{o}C) that was placed between mirrors M2 and M3 (the arm length was 90 mm). The LBO surfaces were AR coated at both λ_{em} and $\lambda_{2\omega}$ wavelengths. The concave mirror M3 has a radius of 50 mm. This arrangement makes use of the high peak power available inside the cavity, and enables high conversion efficiency of the fundamental wavelength λ_{em}.
Figure 5 presents characteristics of the green laser pulses. For a Cr^{4+}:YAG with $T_0 = 0.90$, the maximum average power at 532 nm was 0.95 W (Fig. 5a) at the absorbed pump power of 13.1 W; the laser beam quality was characterized by an M^2 factor of 1.8. The green pulse energy was 226 μJ (Fig. 5b), and the laser runs with a 4.2-kHz rate of repetition and pulse duration of 86 ns. A slightly higher average power of 1.0 W was obtained with the Cr^{4+}:YAG of $T_0 = 0.85$. However, the pulse energy reduced at 131 μJ and the pulse duration increased at 96 ns. Green pulse peak power reached 2.6 kW for the Cr^{4+}:YAG with $T_0 = 0.90$ (Fig. 5b).
The characteristics of Q-switched laser pulses at 532 nm were described with a model of rate equation for photon density inside the resonator (φ), for the inversion of population in

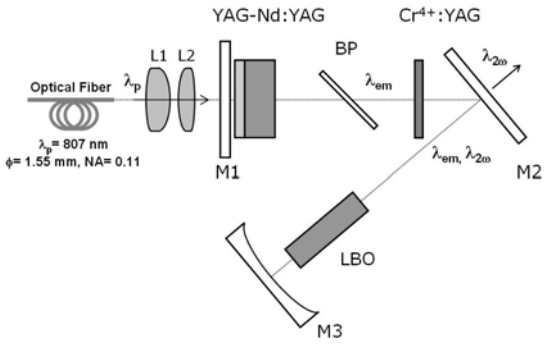

Fig. 4. A passively Q-switched Nd:YAG-Cr^{4+}:YAG laser, intra-cavity frequency doubled by LBO nonlinear crystal.

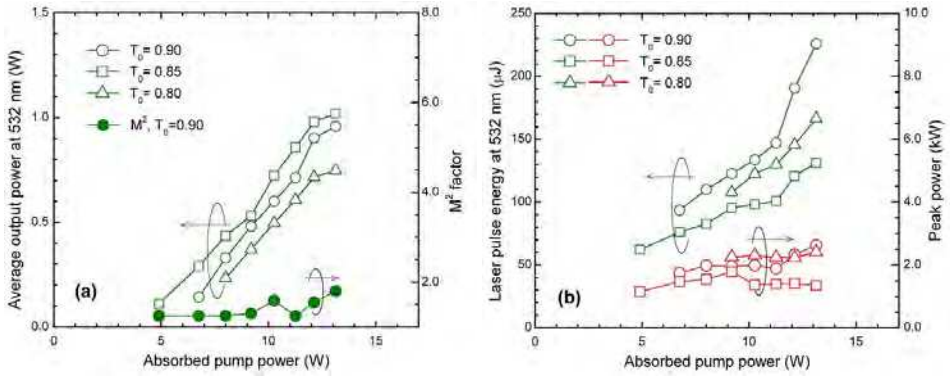

Fig. 5. Characteristics of the laser emission obtained from the Nd:YAG-Cr^{4+}:YAG-LBO laser: (a) Average output power and laser beam M^2 factor; (b) Laser pulse energy and peak power.

Nd:YAG (n_g) and for the population density in Cr^{4+}:YAG (n_{SA}), and in which out-coupling of the cavity field by frequency conversion was considered (Pavel et al., 2001b). The initial population inversion density, n_{gi} is given by relation:

$$n_{gi} = \frac{L - \ln T_0^2}{2\sigma_g \ell_g} \tag{4}$$

The final inversion density n_{gf} and n_{gi} are related by the transcendental equation:

$$\left[1 + \frac{(1-\delta)\cdot \ln T_0^2}{L - \ln T_0^2}\right] \cdot \left[1 - \left(\frac{n_{gf}}{n_{gi}}\right)^d\right] - \frac{d}{d-1} \cdot \frac{n_{gf}}{n_{gi}} \left[1 - \left(\frac{n_{gf}}{n_{gi}}\right)^{d-1}\right] = \frac{(1-\delta)\cdot \ln T_0^2}{L - \ln T_0^2} \cdot \frac{d}{d-\alpha} \cdot \left(\frac{n_{gf}}{n_{gi}}\right)^{\alpha} \cdot \left[1 - \left(\frac{n_{gf}}{n_{gi}}\right)^{d-\alpha}\right] \tag{5}$$

where $d = k/(c\gamma_g\sigma_g)$, and the coefficient k is given by the second-harmonic generation theory (Eimerl, 1987; Honea et al., 1998). The green pulse energy is $E_{2\omega} = h\nu_{2\omega} A \ell_c k \int \varphi^2(t) dt$ with $A_{2\omega}$ the green beam effective area, $h\nu_{2\omega}$ the photon energy at $\lambda_{2\omega}$, and ℓ_c the optical length of the resonator. Finally, the analytical expression deduced for the pulse energy $E_{2\omega}$ was:

$$E_{2\omega}=\frac{h\nu_{2\omega}}{2\gamma_g\sigma_g}\cdot A_{2\omega}\cdot(L-\ln T_0^2)\cdot\left\{\left[1+\frac{(1-\delta)\ln T_0^2}{(L-\ln T_0^2)}\right]\times\ln\frac{n_{gf}}{n_{gi}}+\frac{d}{d-1}\left(1-\frac{n_{gf}}{n_{gi}}\right)\right.$$
$$\left.+\frac{d}{\alpha(d-\alpha)}\cdot\frac{(1-\delta)\ln T_0^2}{(L-\ln T_0^2)}\cdot\left[1-\left(\frac{n_{gf}}{n_{gi}}\right)^{\alpha}\right]-\left[\frac{1}{d(d-1)}+\frac{\alpha}{d(d-\alpha)}\cdot\frac{(1-\delta)\ln T_0^2}{(L-\ln T_0^2)}\right]\times\left[1-\left(\frac{n_{gf}}{n_{gi}}\right)^{d}\right]\right\} \quad (6)$$

Figure 6 shows modeling of the green pulse energy, for the Cr^{4+}:YAG with T_0= 0.90, versus the absorbed pump power, at various values of the losses L. Agreement with experimental results is good, especially if uncertainties in evaluation of L, or of laser beam variation inside the optical resonator are considered.

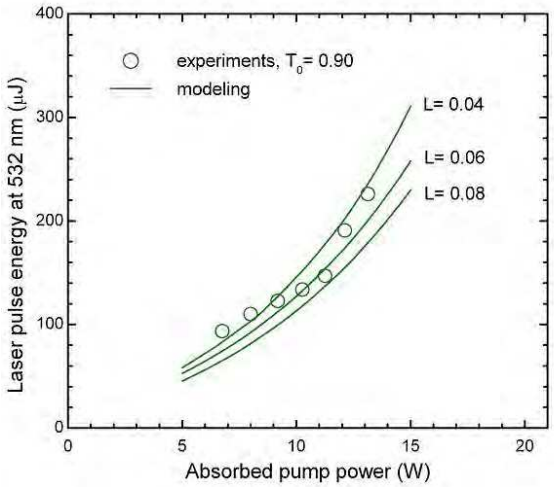

Fig. 6. The green pulse energy versus absorbed pump power for the Cr^{4+}:YAG SA with T_0= 0.90. Signs represent experiments and modeling is given by the continuous lines.

This was the first passively Q-switched Nd:YAG-Cr^{4+}:YAG laser intra-cavity frequency doubled with LBO nonlinear crystal. The laser performances (green pulse of 226 μJ energy and 2.6 kW peak power, with ~1 W average power) were much higher than previously developed systems. For example, green laser pulses with 2.5-μJ energy (190-mW average power) were obtained from a Nd:LSB gain medium passively Q-switched by Cr^{4+}:YAG and intra-cavity frequency doubled by $KTiOPO_4$ (KTP) in a linear resonator (Ostroumov et al., 1997). Furthermore, a Nd:YAG laser that was passively Q-switched by GaAs semiconductor and intra-cavity frequency doubled by KTP, in a V-type laser resonator, yielded green laser pulses with 20.5-μJ energy and ~250-mW average power (Kajava and Gaeta, 1997). Later, a Nd:$GdVO_4$-Cr^{4+}:YAG-KTP laser with 21-μJ energy per pulse (average power of ~400 mW) was realized (Liu et al., 2004). More recently, passively Q-switched Nd:YAG (An et al., 2006) or Nd:$LuVO_4$ lasers (Cheng et al., 2011) intra-cavity frequency doubled with KTP were reported. Novelty of these last two devices is the use of two SA crystals, Cr^{4+}:YAG and GaAs, for the purpose of obtaining shorter and more symmetrical pulses, in comparison with those delivered by a single SA crystal.

3. High-peak power passively Q-switched Nd:YAG/Cr^{4+}:YAG lasers

3.1 Nd:YAG-Cr^{4+}:YAG micro-lasers based on single-crystal components

The cw pumped, passively Q-switched lasers have large pulse-to-pulse energy fluctuations and large timing jitters (Huang et al., 1999; Tang et al., 2003) due to thermal and mechanical instabilities. The purpose of our next research was to realize a Nd:YAG that is passively Q-switched by Cr^{4+}:YAG SA and that can be used for ignition of an automobile engine. The operation frequency of igniters in internal combustion engines is less than 60 Hz, corresponding to an engine speed of 7200 rpm; the duty cycle is less than 5% for automobiles. In such a low frequency range, passively Q-switched lasers that are quasi-cw pumped with a low duty cycle are expected to operate stably due to initialization of the thermal and mechanical conditions during pulses.

Figure 7 is a drawing of a passively Q-switched laser module developed in our laboratory for preliminary experiments (Tsunekane et al., 2008). The active medium was a 1.1-at.% Nd:YAG single crystal (Metal Mining Co., Ltd., Japan) with a length of 4 mm. AR (R<0.2%) and HR (R>99.8%) coatings at λ_p and λ_{em}, respectively, were deposited on the pumped surface S1 of Nd:YAG. HR (R>90%) and AR (R<0.2%) coatings at λ_p and λ_{em}, respectively, were deposited on the intra-cavity surface S2 of Nd:YAG. AR coatings at λ_{em} were deposited on both surfaces of a Cr^{4+}:YAG SA (4-mm thick single crystal; Scientific Materials Corp., USA). The output coupler was flat with transmission T= 0.50 at λ_{em}. Cavity length was 10 mm. The Nd:YAG was end pumped by a fiber coupled, conductive cooled, 120-W peak power laser diode (JOLD-120-QPXF-2P, Jenoptik, Germany) with emission at λ_p= 807 nm; fiber core diameter was 600 μm and numerical aperture NA was 0.22. The fiber end was imaged into Nd:YAG to a spot size of 1.1-mm diameter. Pump energy was controlled by changing the pump pulse duration, whereas the peak pump power was maintained constant at 120 W. The maximum pump duration was 500 μs and the repetition rate was 10 Hz.

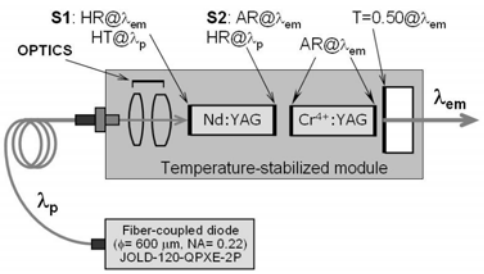

Fig. 7. Schematic drawing of the passively Q-switched Nd:YAG-Cr^{4+}:YAG laser that was build of discrete, Nd:YAG and Cr^{4+}:YAG single crystals.

Figure 8a shows energy of the laser pulse delivered by the Nd:YAG-Cr^{4+}:YAG laser versus initial transmission T_0 of a Cr^{4+}:YAG SA. E_p increases from 0.45 mJ for a Cr^{4+}:YAG with T_0= 0.80 to 4.3 mJ for a Cr^{4+}:YAG with T_0= 0.15. Corresponding pump pulse energy (E_{pump}) was 53 and 5.2 mJ, respectively. The pulse duration was measured with a 10 GHz, InGaAs detector (ET-3500, Electro-Optics Technology, Inc.) and with a 12 GHz oscilloscope (DSO81204B, Agilent Technology). The shortest pulse width of 300 ps was obtained with a Cr^{4+}:YAG of T_0= 0.15 (Fig. 8a). Pulse peak power was 0.16 MW for a Cr^{4+}:YAG with T_0= 0.80 and a record of 14.5 MW for a Cr^{4+}:YAG with T_0= 0.15 (as shown in Fig. 8b).

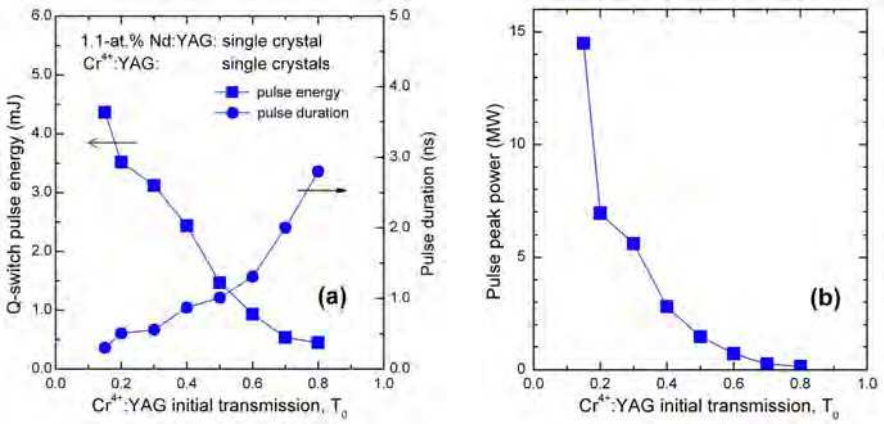

Fig. 8. Characteristics of Q-switched pulses yielded by the Nd:YAG-Cr^{4+}:YAG laser shown in Fig. 7, versus initial transmission T_0 of Cr^{4+}:YAG: a) Energy and duration; b) Peak power.

From the experimental observations, stable breakdown in air was observed for laser pulse energy E_p larger than 1.5 mJ and pulse duration t_p below 1 ns using an aspheric focus lens of 10-mm focal length. Based on these results, a Cr^{4+}:YAG SA single crystal with initial transmission T_0= 0.30 was selected for the laser igniter. The first prototype micro-laser module that was built in our laboratory and that has the same dimensions as a spark plug is shown in Fig. 9. The device includes not only the pumping optics from fiber to the Nd:YAG gain material, but also a beam expanding and focusing optics for ignition. The laser igniter has the same optical design and similar performances as the experimental module shown in Fig. 7, and it is physically possible to ignite a real engine by installing it instead of an electrical spark plug to a plug hole (Tsunekane et al., 2010). For real operation on an engine, however, the mechanical design inside the module has be improved in order to sustain the high temperatures (up to 150°C) and vibrations of a real engine.

Fig. 9. Nd:YAG-Cr^{4+}:YAG laser with one-beam output. Nd:YAG gain medium and Cr^{4+}:YAG SA were single crystals; all optical components (including the output mirror) were discrete elements. Air breakdown is shown and size comparison is made with a spark plug.

3.2 Ceramics versus single-crystals Nd:YAG-Cr^{4+}:YAG micro-lasers

The Nd:YAG as well as the Cr^{4+}:YAG SA media used in the previous reports were single crystals. The advancement in ceramic techniques has reached a maturity stage, especially in obtaining poly-crystalline cubic laser media of very good optical quality. It is recognized that laser ceramics has become a serious challenge to crystalline optics, especially due to an easier manufacturability and a lower price. The use of poly-crystalline ceramics could decrease the price of the Nd:YAG-Cr^{4+}:YAG laser, which is a critical condition for realizing and using of a laser spark plug for engine ignition. We have therefore conducted an investigation of laser output characteristics obtained from a passively Q-switched Nd:YAG-Cr^{4+}:YAG laser that employs single crystals and poli-crystalline ceramics as Nd:YAG active media as well as Cr^{4+}:YAG SA elements.

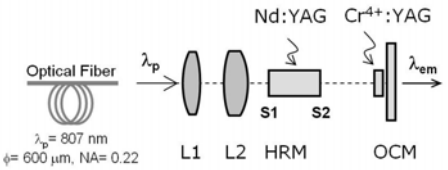

Fig. 10. A sketch of the experimental set-up used for comparative investigation of laser emission with Nd:YAG and Cr^{4+}:YAG single crystals and poly-crystalline ceramics.

A sketch of the experimental set-up is shown in Fig. 10. The laser media were Nd:YAG single crystals with doping level of 1.0-at.% Nd (sample A; Japan) and 2.0-at.% Nd (sample B; Germany), and poly-crystalline Nd:YAG ceramics with 1.1-at.% Nd (sample A*; Baikowski Japan Co., Ltd.) and 2.0-at.% Nd (sample B*; Baikowski Japan Co., Ltd.) doping level. The thickness of sample B* was 3 mm, whereas the other Nd:YAG media had 4 mm in thickness. Side S1 of each Nd:YAG was coated as HR (R> 99.9%) at λ_{em}, and as HT (T> 97%) at λ_p. The other side (S2) was AR coated (T> 99.9%) at λ_{em}, and as HR (R> 95%) at λ_p. The Cr^{4+}:YAG SA had initial transmission, T_0 between 0.80 and 0.20, and were single crystals provided by two different venders (SA1 and SA2, China), as well as poly-crystalline ceramics (SA3; Baikowski Japan Co., Ltd.). Both sides of a Cr^{4+}:YAG SA were AR coated at λ_{em}. Q-switched emission was reported previously in all-ceramics Nd:YAG-Cr^{4+}:YAG (Feng et al., 2004) or Yb:YAG-Cr^{4+}:YAG (Dong et al., 2006; Dong et al, 2007) compact lasers, the pumping being made with diode lasers of low power (few watts) in cw mode. In our experiments, the optical pumping was made with a fiber-coupled diode laser (JOLD-120-QPXF-2P, Jenoptik, Germany) in quasi-cw regime. The pump repetition rate was 10 Hz and the pump pulse duration was fixed at 250 μs; pump energy was controlled by changing the diode current. An optical system made of two L1 and L2 lenses was used to image the fiber end (600-μm in diameter, NA= 0.22) into Nd:YAG to a spot size of 1.1 mm in diameter. A linear resonator made between side S1 of Nd:YAG and a plane OCM was employed.

Figure 11 presents output performances measured in free-generation regime, using a 35-mm long resonator equipped with an OCM of transmission T= 0.20. The slope efficiency, η_s was in the range of 0.65 to 0.61, the highest value being recorded with the 1.0-at.% Nd:YAG single crystal (sample A), as shown in Fig. 11a. The overall optical-to-optical efficiency, η_0 for the maximum pump level of 36.1 mJ per pulse is given in Fig. 11b. Laser pulses with 22.7 mJ energy (optical to optical efficiency η_0 of ~0.63) were measured from the 1.0-at.% Nd:YAG (sample A). Efficiencies η_s and η_0 recorded with the highly-doped Nd:YAG were a

little below those measured with Nd:YAG (single crystals or poly-crystalline ceramics) of low concentrations. On the other hand, each Nd:YAG poly-crystalline ceramics showed a slight decrease of these efficiencies, compared with its counterpart Nd:YAG single crystal.

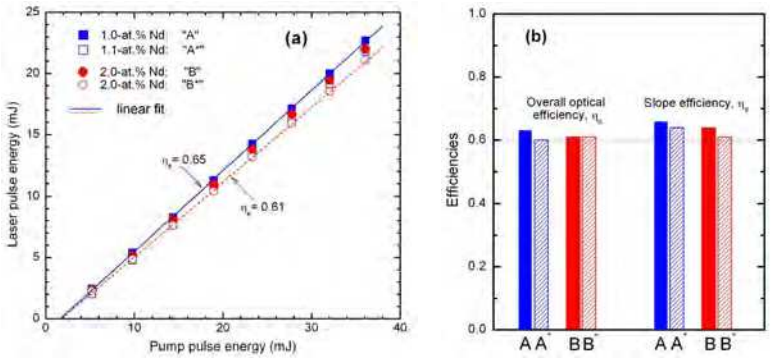

Fig. 11. Characteristics of laser emission in free-generation regime (i.e. without Cr^{4+}:YAG): (a) Laser pulse energy versus pump pulse energy; (b) Overall optical efficiency (η_0) and slope efficiency (η_s) for the available pump pulse energy of 36.1 mJ.

Figure 12 presents characteristics of Q-switched laser pulses obtained with a Cr^{4+}:YAG SA single crystal (SA1) of initial transmission T_0= 0.40, and various OCM transmission T. Laser pulses with energy E_p~1.7 mJ (Fig. 12a) and duration t_p~1.5 ns were yielded by the 1.0-at.% Nd:YAG single crystal (OCM with T= 0.70). The highly-doped 2.0-at.% Nd:YAG single crystal yielded laser pulses with energy E_p= 1.22 mJ and duration t_p= 1.45 ns. The corresponding pulse peak power was 1.1 MW for the 1.0-at.% Nd:YAG and 0.84 MW for the 2.0-at.% Nd:YAG single crystal (Fig. 12c). The Cr^{4+}:YAG single crystal was then replaced with a Cr^{4+}:YAG (SA2) ceramics of the same initial transmission T_0= 0.40. The Q-switched laser pulse energy was E_p= 1.0 mJ for the 1.1-at.% Nd:YAG ceramics (sample A*), and E_p ~1.1 mJ for the 2.0-at.% Nd:YAG ceramics (sample B*) (Fig. 12b). Corresponding pulse peak power was 0.53 and 0.73 MW, respectively. Generally, pulse energy E_p was lower than that measured with the Cr^{4+}:YAG single crystal (SA1), whereas the pulse duration was longer.

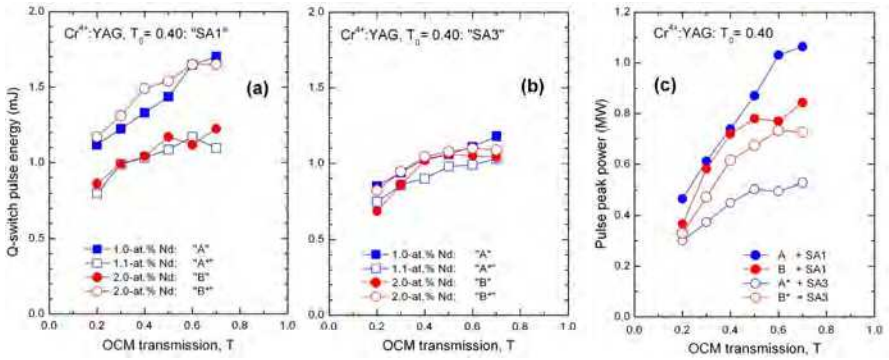

Fig. 12. Q-switched pulse energy versus OCM transmission obtained with Nd:YAG gain media and a Cr^{4+}:YAG SA of T_0= 0.40: (a) The single-crystal Cr^{4+}:YAG (SA1); (b) The poly-crystalline Cr^{4+}:YAG (SA3) ceramics; (c) Laser pulse peak power is shown.

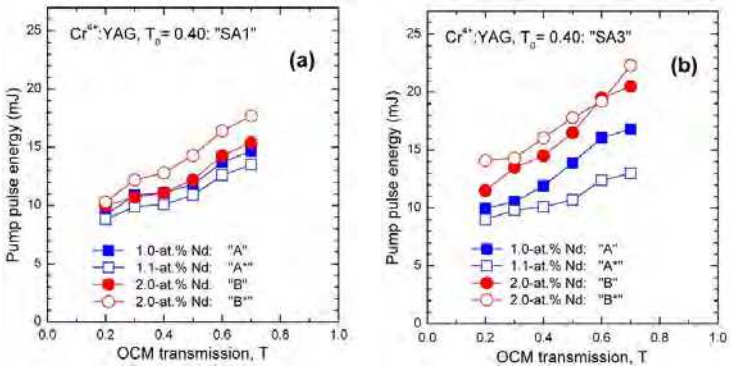

Fig. 13. Pump pulse energy necessary for laser emission with: (a) The single-crystal Cr^{4+}:YAG (SA1); (b) The poly-crystalline Cr^{4+}:YAG (SA3) ceramics.

The pump pulse energy was E_{pump}= 14.7 mJ for 1.0-at.% Nd:YAG (sample A) (Fig. 13a), lower than 15.4 mJ energy of the pump pulse required for Q-switched emission of the 2.0-at.% Nd:YAG sample B (OCM with T= 0.70). On the other hand, E_{pump} necessary for the 1.1-at.% Nd:YAG ceramics (sample A*) was only 13 mJ (Fig. 13b), while E_{pump} required for laser operation of the 2.0-at.% Nd:YAG ceramics was the highest of 22.3 mJ. Generally, higher pump pulse energy was necessary for laser operation of a Nd:YAG gain medium that was Q-switched by Cr^{4+}:YAG ceramics (Fig. 13b), compared with emission of the same laser medium that was Q-switched with a Cr^{4+}:YAG single crystal (Fig. 13a).

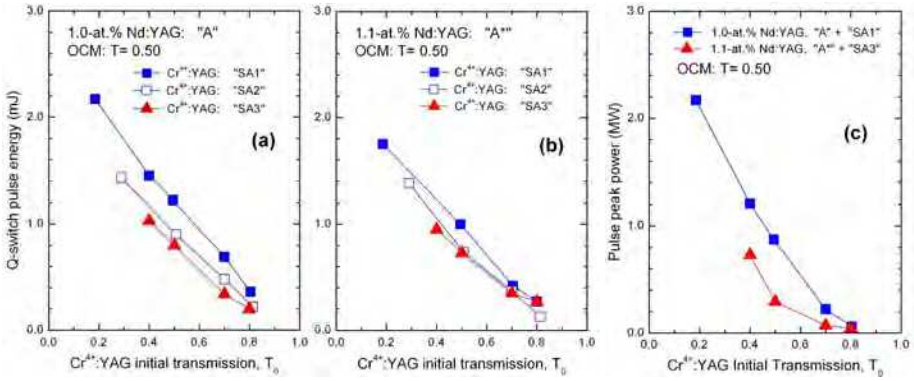

Fig. 14. The influence of Cr^{4+}:YAG initial transmission T_0 on Q-switched laser pulse energy obtained from: (a) The 1.0-at.% Nd:YAG single crystal; (b) The 1.1-at.% Nd:YAG ceramics. (c) Laser pulse peak power is shown.

Figure 14 presents performances of the Q-switched laser pulses obtained with the 1.0-at.% Nd:YAG single crystal (Fig. 14a), the 1.1-at.% Nd:YAG ceramics (Fig. 14b), and using the available Cr^{4+}:YAG SA. The OCM has transmission T= 0.50 and the resonator length was fixed at 35 mm. Differences between pulses obtained with the SA1 and SA2 Cr^{4+}:YAG single crystals were observed at the same initial transmission T_0. Most probably, the final transmissions of the Cr^{4+}:YAG single crystals were a little different, depending of the growth process used by the companies that delivered the SA. Therefore, at this stage of the

experiments (Pavel et al., 2010a) and with the available Nd:YAG gain media and Cr^{4+}:YAG SA components, the best laser performances were obtained with single-crystals elements. The laser pulse peak power (shown in Fig. 14c) was also better when we used Nd:YAG single crystal with Cr^{4+}:YAG single crystal (compared with its counterparts ceramics).

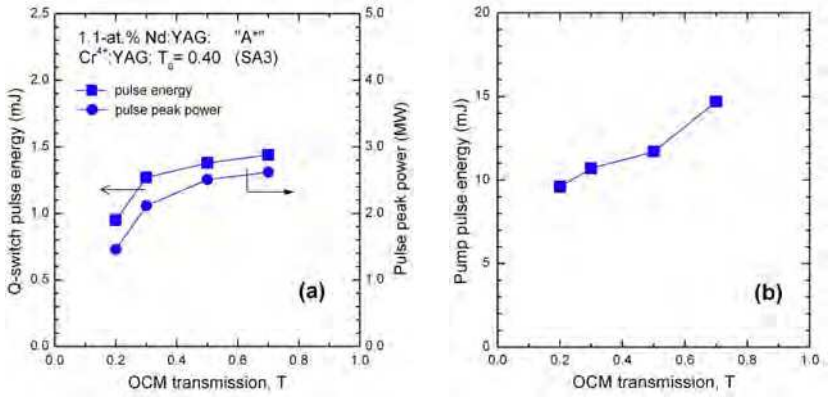

Fig. 15. (a) Q-switched laser pulse energy and peak power versus OCM transmission for the 1.1-at.% Nd:YAG ceramics and the Cr^{4+}:YAG ceramics with T_0= 0.40. The resonator length was 11 mm. (b) Energy of the pump pulse is shown.

In the final experiment the resonator length was reduced to 11 mm. Figure 15 summarizes results obtained with a combination of all-poly-crystalline ceramics, 1.1-at.% Nd:YAG gain medium and Cr^{4+}:YAG SA with T_0= 0.40. Laser pulse energy was around 1.4 mJ when OCM's transmission was higher than T= 0.50, whereas the pulse duration was t_p~ 550 ps. Therefore, corresponding pulse peak power overcomes 2.5 MW (Fig. 15a). Air breakdown was realized with a focusing lens of 11-mm focal length. The pump pulse energy varied between 9.6 mJ when OCM transmission was T= 0.20 (low pulse energy E_p= 0.95 mJ, and t_p= 650 ps) and E_{pump}= 14.7 mJ when OCM transmission was increased at T= 0.70 (Fig. 15b).
It is known that the intensity required for optical breakdown depends on pulse duration. There are not many reports on this subject: According to (Paschotta, 2008), an optical intensity of ~2×10^{13} W/cm^2 is required for air breakdown with laser pulses of 1-ps duration. Therefore, experiments were performed in order to evaluate the optical intensity of ns-duration laser pulses that realizes air breakdown. A Nd:YAG-Cr^{4+}:YAG laser, as shown in Fig. 10, was used. The laser pulse duration was varied by changing the OCM transmission T, and with the help of two Cr^{4+}:YAG that had initial transmission T_0 of 0.39 and 0.29. The resonator length was fixed at 15 mm: The laser beam M^2 factor was ~1.50, as determined by knife-edge method. The air breakdown was observed after a convergent lens of 7.5 mm focal length. A half waveplate and a polarizer were placed after the laser, in order to vary the intensity of the pulse incident on the focusing lens.
Figure 16 presents optical intensity that induced air breakdown (in laboratory conditions). In experiments, the pulse duration t_p could be varied between 0.4 and 1.1 ns; corresponding laser pulse optical intensities that induced air breakdown were ~0.65×10^{13} W/cm^2 and ~0.40×10^{13} W/cm^2, respectively. We therefore concluded that optical intensity of a laser pulse with 1-ns duration that induced air breakdown is ~0.5×10^{13} W/cm^2.

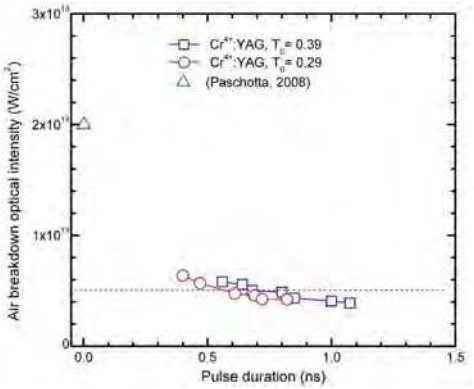

Fig. 16. Optical intensity of a laser pulse with ns duration that induced air breakdown.

3.3 Composite all-ceramics Nd:YAG/Cr^{4+}:YAG monolithic micro-lasers with two and three-beam output for engine ignition

Figure 17 is a sketch of the set-up used to demonstrate, in preliminary experiments, a passively Q-switched Nd:YAG-Cr^{4+}:YAG laser with two-beam output. Generally, one could choose to use one line for pumping, and to divide the high-energy output laser beam into two (ore more) fascicles, which has to be directed at necessary angle and then focused. This solution increases probability of damaging the laser media (due to the high intensity of the laser beam, or due to thermal effects), and could complicate the guiding line. Therefore, our choice was to employ similar, independent, multi-pumping lines, and then to change the optical path of a laser beam before focusing it.

The pump was made at 807 nm (λ_p) with two fiber-coupled (600-μm diameter and numerical aperture NA=0.22) diode lasers (JOLD-120-QPXF-2P, Jenoptik, Germany). Pump repetition rate and pump pulse duration were 5 Hz and 250 μs, respectively. The fiber end was imaged into Nd:YAG to a spot size of 1.1-mm diameter. The two-pump beams were inserted into Nd:YAG with a metal-coated prism. Furthermore, distance between the pumping positions on Nd:YAG input surface was changed by forward and backward translation of this prism.

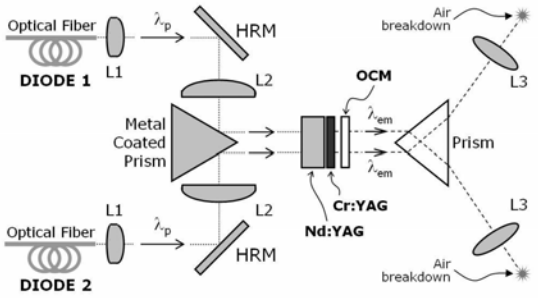

Fig. 17. Schematic of the experimental set-up used for "on table" demonstration of a passively Q-switched Nd:YAG-Cr^{4+}:YAG all-ceramics laser with two-beam output.

The laser medium was a 1.1-at.% Nd:YAG ceramics (Baikowski Japan Co., Ltd.) with thickness of 5 mm and a 10-mm diameter. Surface used for pumping was coated HR at the lasing wavelength of 1.06 μm (λ_{em}) and HT at λ_p. The second surface was coated AR at both λ_{em} and λ_p. Around 90% of the pump radiation was absorbed in Nd:YAG. Cr^{4+}:YAG ceramics with initial transmission T_0 of 0.70, 0.50, and 0.30 were employed for Q-switching, both surfaces of a SA ceramics being coated AR at λ_{em}. The resonator length was 12 mm, and a plane output mirror (OCM) was used for out-coupling. The laser beams path was bent with a prism placed after the resonator, whereas air breakdown was observed behind a lens L3 that has an 11-mm long focal length.

OCM, T	T_0= 0.70			T_0= 0.50			T_0= 0.30		
	E_p (mJ)	t_p (ns)	E_{pump} (mJ)	E_p (mJ)	t_p (ns)	E_{pump} (mJ)	E_p (mJ)	t_p (ns)	E_{pump} (mJ)
0.40	0.8	4.1	9.0	1.0	2.3	12.0	1.7	1.0	18.5
0.50	0.8	2.5	9.5	1.3	1.5	13.0	2.1	0.6	20.0
0.70	0.8	2.4	10.5	1.3	1.4	15.0	2.3	0.7	21.5

Table 1. Characteristics of Q-switched laser pulses obtained from the Nd:YAG-Cr^{4+}:YAG all-poly-crystalline ceramics laser that was build of discrete components.

Characteristics of the Q-switched laser pulses obtained from the Nd:YAG-Cr^{4+}:YAG laser are summarized in Table 1, at various OCM transmission T. Laser pulses of few-ns duration and energy E_p of 0.8 mJ were measured for the Cr^{4+}:YAG with T_0= 0.70. Energy E_p overcame 2 mJ and t_p shortened below 1 ns when combination of Cr^{4+}:YAG with T_0= 0.30 and OCM with T of 0.50 or 0.70 was used. Air breakdown was successfully for the Cr^{4+}:YAG with T_0= 0.30 and all the OCM employed in the experiments.

The next step of our investigations constituted realization of a compact Nd:YAG/Cr^{4+}:YAG laser with two-beam output and dimensions close to an electrical spark plug. Figure 18a shows the experimental set-up. The laser medium was a composite Nd:YAG/Cr^{4+}:YAG ceramics: Research experience of Baikowski Japan Co., as well as available optics on market (for example one could visit: www.thorlabs.com), allowed realization of this medium as a parallelepiped with 10×15 mm^2 surface area, as presented in Fig. 18b. The Nd:YAG doping level was 1.1-at.% Nd, and its length was increased at 8 mm: In this way, the gain medium absorption efficiency at λ_p was better than 0.95, which avoided bleaching effects of Cr^{4+}:YAG by the pump beam (Jaspan et al., 2004). The 3-mm thick Cr^{4+}:YAG SA ceramics had initial transmission T_0= 0.30. Surface S1 of Nd:YAG was coated HR at λ_{em} and HT at λ_p, and the OCM with transmission T= 0.50 was coated on surface S2 of Cr^{4+}:YAG.

The compact pumping line imaged the fiber end to a spot size of 1.0-mm into Nd:YAG. Each laser beam was expanded and then collimated in the "expander" section. Next, the beam was bended with a prism (patent pending), and finally focussed.

The composite, all-ceramics, passively Q-switched Nd:YAG/Cr^{4+}:YAG monolithic laser with two-beam output is shown in Fig. 19a. Figure 19b presents the air breakdown realized with this laser, whereas an electrical spark plug used in industrial gas engine is given for comparison. Each beam delivered Q-switched laser pulses with ~2.5 mJ energy and ~800 ps duration, which corresponds to a peak power of 3.1 MW. Minimal pump pulse energy was ~27 mJ. The laser pulse jitter, which was estimated from 500 consecutive pulses, improved

from 3 μs to 1 μs when the pump pulse energy was increased from 27 mJ to 34 mJ respectively, while the pulse standard deviation decreases from 0.53 μs to 0.18 μs. The prism angle was chose such as the distance between the ignition points (φ_c) was 13 mm, whereas the depth of the ignition (b_c) was 9 mm (Pavel et al., 2011a).

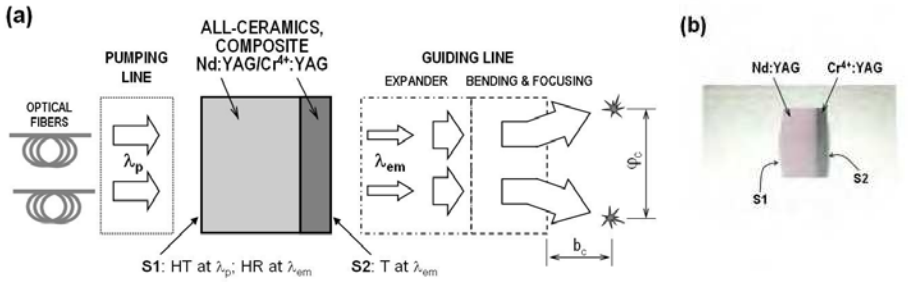

Fig. 18. (a) A sketch of the composite, all-ceramics Nd:YAG/Cr^{4+}:YAG monolithic laser with two-beam output is presented. (b) The rectangular-shaped laser medium is shown.

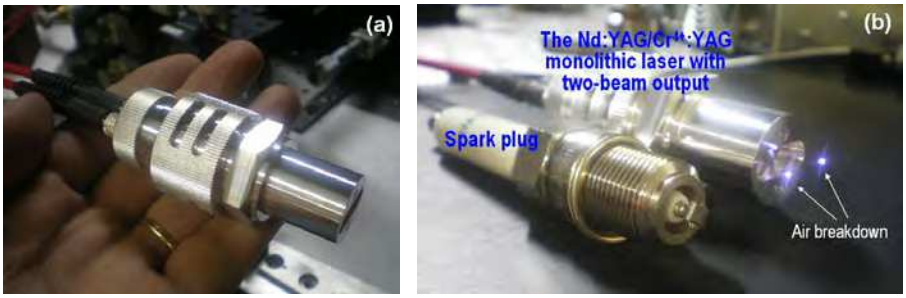

Fig. 19. (a) The Nd:YAG/Cr^{4+}:YAG laser with two-beam output is presented. (b) An electrical spark plug is shown for comparison and air breakdown in two points is illustrated.

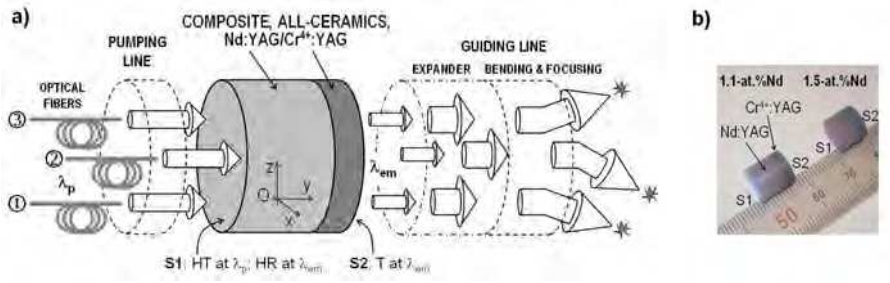

Fig. 20. (a) Schematic of a passively Q-switched, composite, all-ceramics Nd:YAG/Cr^{4+}:YAG monolithic laser with three-beam output. (b) Photo of two composite media is shown.

Once the Nd:YAG/Cr^{4+}:YAG monolithic laser with two-beam output was build, the final goal of our work was realization of a laser device with three-beam output and a size that fits an

electrical spark plug used in automobile industry. The experimental set-up is shown in Fig. 20a. Three composite, all-ceramics Nd:YAG/Cr^{4+}:YAG media (Baikowski Japan Co., Ltd.), each with a 9-mm diameter were prepared for the experiments. While the Cr^{4+}:YAG SA has initial transmission T_0= 0.30 and a thickness of 2.5 mm, the influence of Nd-doping level on Q-switched laser characteristics was investigated by using Nd:YAG with 1.1-at.% Nd (7.5-mm thick), as well as highly-doped 1.5-at.% Nd (thickness of 5 mm) and 2.0-at.% Nd (thickness of 3.5 mm). Again, surface S1 of Nd:YAG was coated HR at λ_{em} and HT at λ_p. The OCM with T= 0.50 at λ_{em} was coated on surface S2 of Cr^{4+}:YAG SA. A photo of two composite Nd:YAG/Cr^{4+}:YAG ceramics is shown in Fig. 20b. The optical pumping was realized through three independent, similar, and compact pumping lines (marked by 1 to 3 in Fig. 20a), each line containing a pair of an aspheric collimating lens and an aspheric focusing lens with short focal length and high NA. We mention that in order to fulfill dimensions of an automobile spark plug, diameter of all lenses was reduced and a new design of the fiber end was made.
The characteristics of the Q-switched laser pulses measured from the Nd:YAG/Cr^{4+}:YAG ceramics are given in Table 2. The energy of the laser pulse yielded by the 1.1-at.% Nd:YAG ceramics was 2.37 mJ, with a pulse peak power of 2.8 MW. The laser beam M^2 factor, which was measured by the knife-edge method, was 3.7.

Nd (at.%)	Pulse energy (mJ)	Pulse duration (ps)	Peak power (MW)	Pump pulse energy (mJ)	M^2 factor
1.1	2.37	850	2.79	27	3.7
1.5	2.03	650	3.12	32.8	4.0
2.0	1.37	660	2.08	32	4.0

Table 2. Characteristics of Q-switched laser pulses obtained from the composite, all-polly-crystalline Nd:YAG/Cr^{4+}:YAG ceramics.

In order to explain the influence of pump-beam spot size on Q-switched laser performances, we used a rate equation model (Zhang et al., 2000; Li et al., 2007) in which the pump beam was assumed to have a top-hat distribution of radius w_p and the laser beam was taken as Gaussian with a spot size of radius w_g. Both w_p and w_g were considered constant along the Nd:YAG/Cr^{4+}:YAG medium. The laser pulse energy is given by Eq. (1), while the initial population inversion density, n_{gi} was written as:

$$n_{gi} = \frac{-\ln R + L - \ln T_0^2}{2\sigma_g \ell_g \cdot \left[1 - \exp\left(-2a^2\right)\right]} \tag{7}$$

with $a = w_p/w_g$. The final population inversion density, n_{gf} and n_{gi} are related by relation:

$$\left(1 - \frac{n_{gf}}{n_{gi}}\right) + \left[1 + \frac{(1-\delta)\cdot \ln T_0^2}{\beta}\right] \cdot \ln\left(\frac{n_{gf}}{n_{gi}}\right) \cdot \frac{(1-\delta)\cdot \ln T_0^2}{\beta} \cdot \left[1 - \left(\frac{n_{gf}}{n_{gi}}\right)^{\alpha}\right] = 0 \tag{8}$$

with parameter β: $\beta = (-\ln R + L - \ln T_0^2)/[1-\exp(-2a^2)]$.
Figure 21 presents n_{gf}/n_{gi} versus ratio $a = w_p/w_g$. In simulation losses were L= 0.06 (0.01 for Nd:YAG and 0.05 for Cr^{4+}:YAG final transmission), while spectroscopic parameter of

Nd:YAG was $\sigma_g = 2.63\times10^{-19}$ cm² (Taira, 2007). If $w_p < w_g$ the overlap between pump and laser beam is good, but n_{gf}/n_{gi} increases when w_p/w_g decreases. Although the initial inversion of population n_{gi} is high, a small fraction of it used for lasing and therefore Q-switched laser pulse energy is low. If w_p/w_g has a large value, the central part of the inversion of population interacts with laser mode, whereas some outside part could be depleted by spontaneous emission. Increasing w_p/w_g decreases n_{gf}/n_{gi}: The final inversion of population is low and a pulse laser with high energy is obtained. The expected values of the Q-switched laser pulse at various sizes w_g of the laser mode were also shown in Fig. 21.

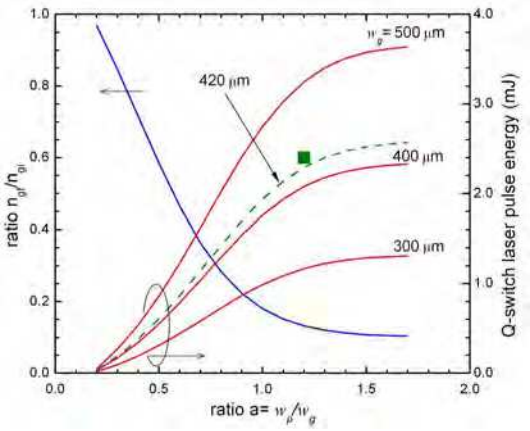

Fig. 21. Ratio n_{gf}/n_{gi} versus w_p/w_g and Q-switched laser pulse energy for various laser beam radii w_g. The pulse energy obtained from the 1.1-at.% Nd:YAG is given by the sign (■).

A plane-plane resonator operates due to thermal effects induced by optical pumping in the laser medium. The focal length f of Nd:YAG thermal lens can be evaluated by relation: $f = (\pi K_c w_p^2)/[P_h \cdot (dn/dT)]$ (Innocenzi et al., 1990). Nd:YAG has thermal conductivity K_c= 10.1 $Wm^{-1}K^{-1}$ (Sato & Taira, 2006), thermal coefficient of the refraction index is $dn/dT = 0.73\times10^{-5}$ K^{-1}, while ~0.24 of the absorbed pump power is transformed into heat (P_h) under efficient laser emission at 1.06 μm. The average thermal lens of the 1.1-at.% Nd:YAG was evaluated as ~6.5 m, whereas value of w_g was determinate by an ABCD description of the resonator as ~420 μm. Sign of Fig. 21 is the experimental value of the laser pulse energy obtained from the 1.1-at.% Nd:YAG. Agreement with theoretical modeling is good, especially if uncertainties in evaluation of thermal focal lens or of other system parameters (such as losses L) are considered. The model can be improved by taking into account variation of pump beam radius w_p and of laser beam spot size w_g along the resonator length.

Energies of 2.03 mJ and 1.37 mJ were measured from the 1.5-at.% and 2.0-at.% Nd ceramics, respectively. The pump pulse energy increased from 27 mJ for the 1.1-at.% Nd:YAG to 33 mJ for the 1.5-at.% Nd:YAG, and to 32 mJ for the 2.0-at.% Nd:YAG. The decrease of the $^4F_{3/2}$ upper-level lifetime with Nd-doping level could be a reason for lower laser performances recorded with the highly-doped Nd:YAG compared with the 1.1-at.% Nd:YAG. The OCM transmission has also to be optimized for the highly-doped Nd:YAG ceramics.

Nd (at.%)	Average pulse energy (mJ)		Standard deviation (mJ)	
	Ox	Oz	Ox	Oz
1.1	2.36	2.34	0.02	0.06
1.5	2.03	2.03	0.03	0.03
2.0	1.33	1.34	0.05	0.02

Table 3. Average laser pulse energy and standard deviation measured along Ox and Oz axis of the Nd:YAG/Cr^{4+}:YAG ceramics media.

Very important for performances of the monolithic laser is the uniformity of the ceramic Nd:YAG/Cr^{4+}:YAG material. Table 3 presents average values of the laser pulse energy determined along Ox and Oz axes, estimated by scanning the medium with a 0.5-mm step. The laser pulse energies were very close to those measured at the media center. Moreover, standard deviation was small, below 3% for the 1.1-at.% Nd:YAG, and less than 4% for the highly-doped Nd:YAG. The results indicate a very good homogeneity as well as quality of the composite all-ceramics Nd:YAG/Cr^{4+}:YAG media, in spite of the high, 9-mm diameter. As an example, laser pulse energy measured from the highly-doped, 2.0-at.% Nd:YAG/Cr^{4+}:YAG medium is given in Fig. 22.

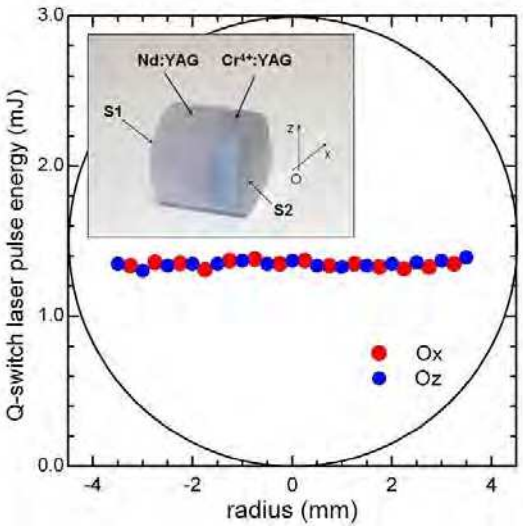

Fig. 22. Laser pulse energy measured along horizontal and vertical axis of the 2.0-at.% Nd:YAG/Cr^{4+}:YAG ceramics (inset shows the composite medium).

The three-beam output micro-laser (Fig. 23a) was realized with the composite, all-ceramics 1.1-at.% Nd:YAG/Cr^{4+}:YAG medium. The guiding line (Pavel et al., 2011b) was designed to assure a distance between a focusing point and the laser axis, φ_c of 4.5 mm and a depth of the focusing point inside the combustion chamber, b_c of 9 mm. Air breakdown is illustrated in Fig. 23b, and an automobile electrical spark plug is shown for comparison.

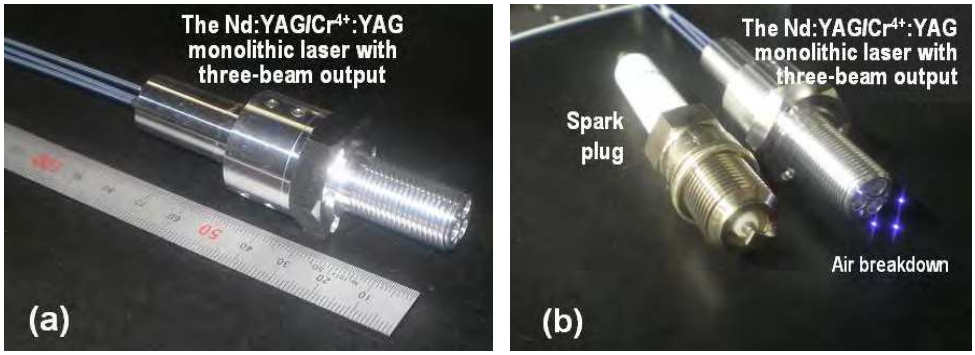

Fig. 23. (a) The passively Q-switched Nd:YAG/Cr^{4+}:YAG micro-laser with three-beam output is shown. (b) Air breakdown in three points is realized.

Various other characteristics of a Q-switched laser pulse, such us the delay time (i.e. the time between the moment when the pump pulse begins and the moment when the laser pulse develops), or the pulse jitter and standard deviation were determined. Figure 24 presents these parameters function of the pump pulse energy. As expected, delay time decreases with the increase of the pump pulse power. Therefore, the use of independent pumping lines allows control of the air breakdown timing by changing the pump energy of each line. Furthermore, real simultaneous ignition in all three points can be obtained by a small (less than 5%) tuning of the pump energy of each individual line. Time jitter is low (2.1 μs at the pump energy of 26.7 mJ and 1.0 μs at 32-mJ available energy of the pump pulse) and thus it would not have a negative impact on an automobile engine that is ignited by the laser. A second laser pulse was not observed. Nevertheless, increasing the pump pulse duration would enable obtaining of multiple laser pulses (Weinrotter et al., 2005; Tsunekane et al., 2010), which are useful for engine ignition especially if lean fuel-air mixtures are used.

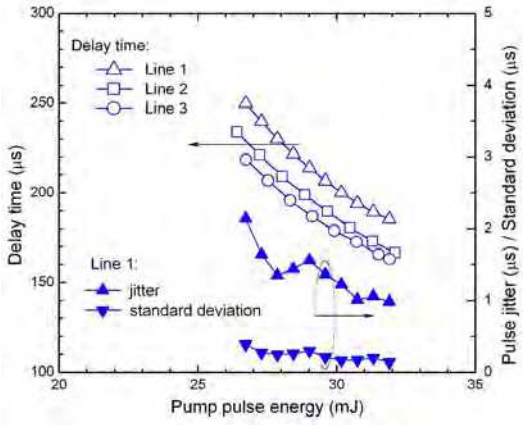

Fig. 24. Time delay of the Q-switched laser pulse, and time jitter and standard deviation versus pump pulse energy, for the repetition rate of 5 Hz (250-μs pump pulse duration).

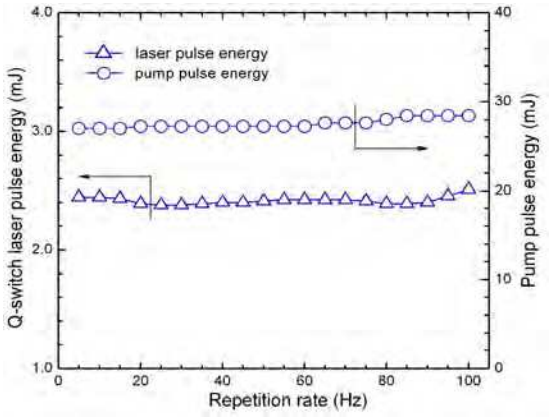

Fig. 25. Q-switched laser pulse energy and pump pulse energy versus pump repetition rate.

Previous experiments were performed at 5-Hz pump repetition, and temperature of the composite Nd:YAG/Cr^{4+}:YAG ceramics was not controlled. However, higher repetition rates are necessary for operation of a car engine, usually up to 60 Hz. Therefore, variation of laser pulse characteristics was investigated versus the pump repetition rate. Experiments concluded that an increase from 5 to 100 Hz of the pump repetition rate improved the laser pulse energy from 2.37 mJ to 2.51 mJ, i.e. by only a 6% fraction, as shown in Fig. 25. This change required a small (5 to 6%) increase of the minimal pump energy, from ~27 mJ at 5 Hz pump repetition rate to 28.4 mJ at the pump repetition rate of 100 Hz. Variation with temperature of the laser performances was behind this work purpose. Nevertheless, in prior papers (Tsunekane and Taira, 2009; Dascalu and Pavel, 2009; Pavel et al., 2010b) we have measured only a slight increase of the laser pulse energy when temperature of a Nd:YAG laser passively Q-switched by Cr^{4+}:YAG SA (build of discrete, single-crystals components) was increased up to 150^{o}C. Future experiments would also consider testing of the laser to shock and vibration conditions that are similar to those experienced in a car engine.

4. Conclusion

A passively Q-switched Nd:YAG/Cr^{4+}:YAG giant-pulse emitting micro-laser with up to three-beam output has been realized. The device incorporates a composite, all-ceramics Nd:YAG/Cr^{4+}:YAG monolithic structure that was pumped by similar, independent lines. The laser size is comparable to that of an electrical spark plug, being the first demonstration of this kind of device to the best of our knowledge. Laser pulses with energy of ~2.4 mJ and 2.8-MW peak power at 5-Hz repetition rate were obtained from a 10-mm thick Nd:YAG/Cr^{4+}:YAG ceramics, just such as "giant micro-photonics". Increasing pump repetition rate up to 100 Hz improved the laser pulse energy by 6% and required only a 6% increase of the pump pulse energy compared with operation at 5 Hz. Pulse timing of the laser beams can by controlled by changing the pump energy of each individual line. On the other hand, simultaneous multi-point ignition is possible by less than 5% tuning of the pump energy of each individual pump line. These lasers will enable studies on the performances of internal combustion engines with multi-point ignition.

5. Acknowledgment

This work was financed by Japan Science and Technology Agency, and partially supported by DENSO Company, Japan. Permanent support from and fruitful discussions with Mr. Kenji Kanehara of Nippon Soken. Inc. is acknowledged.The authors thank Mr. Nobuo Mizutani of IMS Equipment Development Division for the help with the laser module design. N. Pavel acknowledges partial support of the Romanian Ministry of Education and Research, project 12106/01.10.2008.

6. References

Agnesi, A.; Dell'Acqua, S. & Reali, G. C. (1997). 1.5 Watt passively Q-switched diode-pumped cw Nd:YAG laser. *Opt. Commun.,* Vol. 133, No. 1-6, pp. 211-215.

An, J; Zhao, S. Z.; Li, G. Q.; Yang, K. J.; Sun, Y. M.; Li, D. C.; Wang, J. & Li, M. (2006). Doubly passively Q-switched intracavity-frequency-doubling Nd^{3+}:YAG/KTP green laser with GaAs and Cr^{4+}: YAG saturable absorbers. *Opt. Eng.*, Vol. 45, No.12, Art. No. 124202.

Aniolek, K. W.; Schmitt, R. L.; Kulp, T. J.; Richman, B. A.; Bisson, S.E. & Powers, P. E. (2000). Microlaser-pumped periodically poled lithium niobate optical parametric generator-optical parametric amplifier. *Opt. Lett.* Vol. 25, No. 8, pp. 557-559.

Bibeau, C.; Beach, R. J.; Mitchell, S. C.; Emanuel, M. A.; Skidmore, J.; Ebbers, C. A.; Sutton, S. B. & Jancaitis, K. S. (1998). High-average-power 1-μm performance and frequency conversion of a diode-end-pumped Yb:YAG laser. *IEEE J. Quantum Electron.,* Vol. 34, No. 10, pp. 2010-2019.

Cheng, K.; Zhao, S.; Li, Y.; Li, G.; Li, D., Yang, K.; Zhang, G.; Ge, H. & Yu, Z. (2011). Diode-pumped doubly passively Q-switched Nd:$LuVO_4$/KTP green laser with Cr^{4+}:YAG and GaAs saturable absorbers. *Opt. Commun.,* Vol. 284, No. 1, pp. 344-349.

Dascalu, T. & Pavel, N. (2009). High-temperature operation of a diode-pumped passively Q-switched Nd:YAG/Cr^{4+}:YAG laser. *Laser Phys.* Vol. 19, No. 11, pp. 2090-2095.

Degnan, J. (1995). Optimization of passively Q-switched lasers. *IEEE J. Quantum Electron.*, Vol. 31, No. 11, pp. 1890-1901.

Dong, J.; Shirakawa, A.; Takaichi, K.; Ueda, K.; Yagi, H.; Yanagitani, T. & Kaminskii, A.A. (2006). All-ceramic passively Q-switched Yb:YAG/Cr^{4+}:YAG microchip laser. *Electron. Lett.,* Vol. 42, No. 20, pp. 1154-1156.

Dong, J.; Ueda, K.; Shirakawa, A.; Yagi, H.; Yanagitani, T. & Kaminskii, A.A. (2007). Composite Yb:YAG/Cr^{4+}:YAG ceramics picosecond microchip lasers. *Opt. Express*, Vol. 15, No. 22, pp. 14516-14523.

Eimerl, D. (1987). High average power harmonic generation. *IEEE J. Quantum Electron.,* Vol. 23, No. 5, pp. 575-592.

Feng, Y.; Lu, J.; Takaichi, K.; Ueda, K.; Yagi, H.; Yanagitani, T. & Kaminskii, A.A. (2004). Passively *Q*-switched ceramic Nd^{3+}:YAG/Cr^{4+}:YAG lasers. *Appl. Opt.,* Vol. 43, No. 14, pp. 2944-2947.

Hanson, F. (1995). Improved laser performance at 946 and 473 nm from a composite Nd:$Y_3Al_5O_{12}$ rod. *Appl. Phys. Lett.*, Vol. 66, No. 26, pp. 3579-3551.

Honea, E. C.; Ebbers, C. A.; Beach, R. J.; Speth, J. A.; Skidmore, J. A.; Emanuel, M. A. & Payne, S. A. (1998). Analysis of an intracavity-doubled diode-pumped *Q*-switched Nd:YAG laser producing more than 100 W of power at 0.532 mm. *Opt. Lett.*, Vol. 23, No. 15, pp. 1203-1205.

Huang, S.; L.; Tsui; T.; Y., Wang, C. H. & Kao, F. J. (1999). Timing jitter reduction of a passively Q-switched laser, *Jpn. J. Appl. Phys.*, Vol. 38, Part 2, No. 3A, pp. L239-241.

Innocenzi, M. E.; Yura, H. T.; Fincher, C. L. & Fields, R. A. (1990). Thermal modeling of continuous-wave end-pumped solid-state lasers. *Appl. Phys. Lett.* Vol. 56, No. 19, pp. 1831-1833.

Jaspan, M. A.; Welford, D. & Russell, J. A. (2004). Passively Q-switched microlaser performance in the presence of pump-induced bleaching of the saturable absorber. *Appl. Opt.,* Vol. 43, No. 12, pp. 2555-2560.

Kajava, T. T & Gaeta, A. L. (1997). Intra-cavity frequency-doubling of a Nd:YAG laser passively *Q*-switched with GaAs . *Opt. Commun.,* Vol. 137, No. 1-2, pp. 93-97.

Kofler, H.; Tauer, J.; Tartar, G.; Iskra, K.; Klausner, J.; Herdin, G. & Wintner, E. (2007). An innovative solid-state laser for engine ignition. *Laser Phys. Lett.,* Vol. 4, No. 4, pp. 322-327.

Kroupa, G.; Franz, G. & Winkelhofer, E. (2009). Novel miniaturized high-energy Nd:YAG laser for spark ignition in internal combustion engines. *Opt. Eng.,* Vol. 48, No. 1, art. 014202 (5 pages).

Li, S. T.; Zhang, X. Y.; Wang, Q. P.; Li, P.; Chang, J.; Zhang, X. L. & Cong, Z. H. (2007). Modeling of Q-switched lasers with top-hat pump beam distribution. *Appl. Phys. B,* Vol. 88, No. 2, pp. 221-226.

Liu, J.; Yang, J. & He, J. (2004). Diode-pumped passively Q-switched intracavity frequency doubled Nd:$GdVO_4$/KTP green laser. *Opt. & Laser Techn.,* Vol. 36, No. 1, pp. 31-33.

Ma, J. X.; Alexander, D. R. & Poulain, D. E. (1998). Laser spark ignition and combustion characteristics of methane-air mixtures. *Comb. Flame,* Vol. 112, No. (4), pp. 492-506.

Morsy, M. H.; Ko, Y. S.; Chung, S. H. & Cho, P. (2001). Laser-induced two-point ignition of premixture with a single-shot laser. *Comb. Flame,* Vol. 125, No. 4, pp. 724-727.

Ostroumov, V. G.; Heine, F.; Kück, S; Huber, G; Mikhailov, V. A. & Shcherbakov, I. A. (1997). Intracavity frequency-doubled diode-pumped Nd: $LaSc_3(BO_3)_4$ lasers. *Appl. Phys. B,* Vol. 64, No. 3, pp. 301-3.5.

Paschotta, R. (2008). Encyclopedia of Laser Physics and Technology. Handbook/Reference Book. ISBN-10: 3-527-40828-2, ISBN-13: 978-3-527-40828-3; 2008 WILEY-VCH Verlag GmbH & Co. KGaA, Weinheim.

Pavel, N.; Saikawa, J. & Taira, T. (2001b). Diode end-pumped passively Q-switched Nd:YAG laser intra-cavity frequency doubled by LBO crystal. *Opt. Commun.,* Vol. 195, No. 1-4, pp. 233-240.

Pavel, N.; Saikawa, J.; Kurimura, S. & Taira, T. (2001a). High average power diode end-pumped composite Nd:YAG laser passively Q-switched by Cr^{4+}:YAG saturable absorber. *Jap. J. Appl. Phys.,* Vol. 40, Part. 1, No. 3A, pp. 1253-1259.

Pavel, N.; Tsunekane, M. & Taira, T. (2010a). High peak-power passively Q-switched all-ceramics Nd:YAG/Cr^{4+}:YAG lasers. Proceedings SPIE, Vol. 7469, Micro- to Nano-Photonics II - ROMOPTO 2009 Conference, 31 August – 03. Sept., 2009, Sibiu, Romania; paper 746903.

Pavel, N.; Tsunekane, M.; Kanehara, K. & Taira, T (2011a). Composite all-ceramics, passively Q-switched Nd:YAG/Cr^{4+}:YAG monolithic micro-laser with two-beam output for multi-point ignition. In: *CLEO 2011, Laser Science to Photonics Applications Conference*, Baltimore, Maryland, USA, 1-6 May, 2011, paper CMP1.

Pavel, N; Tsunekane, M. & Taira, T. (2010b). Enhancing performances of a passively Q-switched Nd:YAG/Cr^{4+}:YAG microlaser with a volume Bragg grating output coupler. *Opt. Lett.* Vol. 35, No. 10, pp. 1617-1619.

Pavel, N; Tsunekane, M. & Taira, T. (2011b). Passively Q-switched Nd:YAG/Cr^{4+}:YAG all-ceramics, composite, monolithic micro-lasers with multi-beam output for laser ignition. In: *CLEO Europe - EQEC 2011 Conference*, Münich, Germany, 22-26 May, 2011, paper CA7.1.

Phuoc, T. X. & White, F. P. (1999). Laser-induced spark ignition of CH_4/Air mixtures. *Comb. Flame,* Vol. 119, No. 3, pp. 203-216.

Phuoc, T. X. (2000). Single-point versus multi-point laser ignition: Experimental measurements of combustion times and pressures. *Comb. Flame,* Vol. 122, No. 4, pp. 508-510.

Sakai, H.; Kan, H. & Taira T., (2008). >1 MW peak power single-mode high-brightness passively Q-switched Nd^{3+}:YAG microchip laser. *Opt. Express,* Vol. 16, No. 24, pp. 19891-19899.

Sato, Y. & Taira, T. (2006). The studies of thermal conductivity in $GdVO_4$, YVO_4, and $Y_3Al_5O_{12}$ measured by quasi-one-dimensional flash method. *Opt. Express*, Vol. 14, No. 22, pp. 10528-10536.

Shimony, Y.; Burshtein, Z. & Kalisky, Y. (1995). Cr^{4+}:YAG as passive Q-switch and Brewster plate in a pulsed Nd-laser. *IEEE J. Quantum Electron.,* Vol. 31, No. 10, pp. 1738-1741.

Song, J.; Li, C.; Kim, N. S. & Ueda, K. I. (2000). Passively Q-switched diode-pumped continuous-wave Nd:YAG–Cr^{4+}:YAG laser with high peak power and high pulse energy. *Appl. Opt*., Vol. 39, No. 27, pp. 4954-4958.

Taira, T. (2007). RE^{3+}-ion-deped YAG ceramic lasers. *IEEE J. Sel. Top. Quantum Electron.*, Vol. 13, No. 3, pp.798-809.

Tang, D. Y.; Ng, S. P.; Qin, L. J. & Meng, X. L. (2003). Deterministic chaos in a diode-pumped Nd:YAG laser passively Q switched by a Cr^{4+}:YAG crystal, *Opt. Lett*., Vol. 28, No. 5, pp. 325-327.

Tsunekane, M. & Taira, T. (2009). Temperature and polarization dependences of Cr:YAG transmission for passive Q-switching. In: *Conference on Lasers and Electro-Optics/International Quantum Electronics Conference*, Baltimore, Maryland, USA, May 31 - June 5, 2009, paper JTuD8.

Tsunekane, M.; Inohara, T.; Ando, A.; Kanehara, K. & Taira, T. (2008). High peak power, passively Q-switched Cr:YAG/Nd:YAG micro-laser for ignition of engines. In: *Advanced Solid-State Photonics*, OSA Technical Digest Series (CD) (Optical Society of America, 2008); 27-30 January, 2008, Nara, Japan, paper MB4.

Tsunekane, M.; Inohara, T.; Ando, A.; Kido, N.; Kanehara, K. & Taira, T. (2010). High peak power, passively Q-switched microlaser for ignition of engines. *IEEE J. Quantum Electron.,* Vol. 46, No. 2, pp. 277-284.

Tsunekane, M.; Taguchi, N.; Kasamatsu, T. & Inaba, H. (1997). Analytical and experimental studies on the characteristics of composite solid-state laser rods in diode-end-pumped geometry. *IEEE J. Sel. Top. Quantum Electron*., Vol. 3, No. 1, pp. 9-18.

Weinrotter, M.; Kopecek, H. & Wintner, E. (2005b). Laser ignition of engines. *Laser Phys.,* Vol. 15, No. 7, pp. 947-953.

Weinrotter, M.; Kopecek, H.; Tesch, M.; Wintner, E; Lackner, M. & Winter, F. (2005a). Laser ignition of ultra-lean methane/hydrogen/air mixtures at high temperature and pressure," *Exp. Therm. Fluid Science,* Vol. 29, No. 8, pp. 569-577.

Zayhowski, J.; Cook, C. C.; Wormhoudt, J. & J. H. Shorter, J. H. (2000). Passively Q-switched 214.8-nm Nd:YAG/Cr^{4+}:YAG microchip-laser system for the detection of NO. In *Advanced Solid State Lasers*, OSA Technical Digest Series (Optical Society of America, 2000), Davos, Switzerland, Feb. 2000, paper WB4.

Zayhowsky, J. J. & Dill III, C. (1994). Diode-pumped passively Q-switched picosecond microchip lasers. *Opt. Lett*., Vol. 19, No. 18, pp. 1427-1429.

Zhang, X.; Zhao, S., Wang, Q., Zhang, Q., Sun, L. & Zhang, S. (1997). Optimization of Cr^{4+}-doped saturable-absorber Q-switched lasers, *IEEE J. Quantum Electron*., Vol. 33, No. 12, pp.2286-2294.

Zhang, X.; Zhao, S.; Wang, Q.; Ozygus, B. & Weber, H. (2000). Modeling of passively Q-switched lasers. *J. Opt. Soc. Am. B*., Vol. 17, No. 7, pp. 1166-1175.

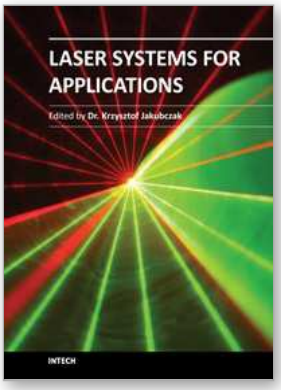

Laser Systems for Applications

Edited by Dr Krzysztof Jakubczak

ISBN 978-953-307-429-0
Hard cover, 308 pages
Publisher InTech
Published online 14, December, 2011
Published in print edition December, 2011

This book addresses topics related to various laser systems intended for the applications in science and various industries. Some of them are very recent achievements in laser physics (e.g. laser pulse cleaning), while others face their renaissance in industrial applications (e.g. CO2 lasers). This book has been divided into four different sections: (1) Laser and terahertz sources, (2) Laser beam manipulation, (3) Intense pulse propagation phenomena, and (4) Metrology. The book addresses such topics like: Q-switching, mode-locking, various laser systems, terahertz source driven by lasers, micro-lasers, fiber lasers, pulse and beam shaping techniques, pulse contrast metrology, and improvement techniques. This book is a great starting point for newcomers to laser physics.

InTech Europe
University Campus STeP Ri
Slavka Krautzeka 83/A
51000 Rijeka, Croatia
Phone: +385 (51) 770 447
Fax: +385 (51) 686 166
www.intechopen.com

InTech China
Unit 405, Office Block, Hotel Equatorial Shanghai
No.65, Yan An Road (West), Shanghai, 200040, China
中国上海市延安西路65号上海国际贵都大饭店办公楼405单元
Phone: +86-21-62489820
Fax: +86-21-62489821